

# Formation of Stellar Streams Due to the Decay of Star Clusters, OB Associations, and Galaxy Satellites

A. V. Tutukov<sup>a</sup>, M. D. Sizova<sup>a, \*</sup>, and S. V. Vereshchagin<sup>a</sup>

<sup>a</sup> *Institute of Astronomy, Russian Academy of Sciences, Moscow, 119017 Russia*

\**e-mail: sizova@inasan.ru*

Received May 8, 2020; revised May 18, 2020; accepted May 30, 2020

**Abstract**—This paper presents a scenario of the evolution of OB associations and star clusters from formation to decay, in the process of which they turn into stellar streams moving in the disk and stellar “rings” around the galactic center. The scenario also includes the formation of stellar streams by galaxies absorbing their dwarf satellite galaxies. The simplest spatial kinematic models of evolution are constructed. It is shown that the stellar structures that appear in the models are similar to the observed stellar streams.

DOI: 10.1134/S106377292010008X

## 1. INTRODUCTION

The study of the physics and evolution of star clusters is one of the primary fields of stellar astronomy. More than 10000 articles have been dedicated to this problem over the past hundred years. Currently, the research results in this area are presented annually in approximately 500 ADS articles (Astrophysics Data System, [http://adsabs.harvard.edu/ads\\_abstracts.html](http://adsabs.harvard.edu/ads_abstracts.html)). There are several reasons for the constant active interest of astronomers in the statistics, physics, and evolution of star clusters. The studies of different-aged clusters turned these astronomical objects into an effective and largely irreplaceable tool for understanding the evolution of stars and galaxies. The study of the star motion in clusters and the motion of the clusters themselves in the Galaxy has become the basis for examining the distribution of mass in clusters and galaxies.

The history of the study of star clusters is an essential part of astronomy history itself. Even Democritus and Anaxagoras identified light spots in the sky as dense groups of stars indistinguishable to the naked eye. After Galileo introduced the telescope into astronomical practice, this allowed Messier (1781) [1] and W. Herschel (1786) [2] to start compiling the first catalogs that included star clusters. The growing accuracy of observational instruments enabled an astrometric estimation of distances to nearby stars (J. Herschel, 1815) [3] and over time allowed updating the data on star clusters (Dreyer, 1888) [4]. As early as the end of the 19th century, it was clear that the decay of star clusters led to the occurrence of stellar streams in the Galaxy (Proctor, 1869) [5]. Such streams themselves were discovered later; as we will see below, the study of their properties is currently given much attention.

At the beginning of the 20th century, the luminosity function (Fleming, 1904) [6] and the dynamics of stars in clusters [7, 8] became subjects of active study. In the 1930s, it became possible to estimate the masses of star clusters based on spectroscopy of the constituent stars (Shapley, 1930) [9]. In 1913, Chandrasekhar showed [10] that gravitationally bound clusters are unstable, and their stars “evaporate” over time as a result of pairwise interactions, leaving the clusters.

The study of star clusters had a decisive role in the formation of basic views on stellar evolution. The Hertzsprung–Russell diagram turned out to be a reliable and convenient tool for determining the age of clusters and understanding their evolution. The role of nuclear reactions as a source of star energy was proved (e.g., Eddington, 1920 [11]), which in turn allowed the first models of the Sun (Gamow, 1938 [12]; Schwarzschild, 1943 [13]) and other stars (Bondi and Bondi, 1951) [14] to be constructed. The study of various sources of nuclear energy inside stars led to the establishment of a physically determined picture of stellar evolution dependent on the star mass. The “standard candle” of the main sequence of open star clusters still remains a reliable measure of their age, as well as the age of galaxies and the universe itself (Zwicky, 1960) [15].

The question of the origin and evolution of star clusters and OB associations incorporating them has an interesting history. The concept of continuous star formation in the Galaxy was proposed by W. Herschel [16]. The idea of the gravitational instability (Jeans, 1902) [17] as the cause of the star formation was easily generalized to the formation of clusters, OB associations, and galaxies (Hoyle, 1953) [18]. In 1946, Blaauw [19] assembled a complete catalog of radial

and tangential velocities of massive stars in the nearby star formation regions. As a result, he came to the conclusion of instability in star formation zones. The spatial dimensions of such systems span hundreds of parsecs. In 1951, V.A. Ambartsumian studied the velocities of young stars in OB associations and found them to be gravitationally unstable. This contradicted simple views on the gravitational instability of a system with initial negative energy as the cause of the occurrence of OB associations. To explain the obvious contradiction with the gravitational instability scenario, Ambartsumian suggested that stars and OB associations, same as our Universe, form due to the decay of some superdense D-bodies. It should be noted that such phenomena as D-bodies (Ambarzumjan, 1951) [20], dark matter (Zwicky, 1953) [21], and dark energy (Perlmutter et al., 1999) [22] were invoked in astrophysics in cases when current ideas did not allow the comprehension of a new phenomenon. The above three cases were based on subsequently resolved paradoxes of estimating spatial velocities, masses of galaxies, and type I supernova brightnesses.

This paper proposes a scenario for solving the paradox of decaying OB associations and clusters in the context of the galactic disk kinematics. To illustrate the scenario, at the end of the paper, we provided the numerical calculation results demonstrating the evolution of the considered stellar systems in a simple model, and included the distributions of the apparent stellar density in the IC 2391 cluster.

## 2. FORMATION OF PROTOCLUSTERS

The formation of OB associations in spiral galaxies is an example of the galactic gas disk fragmentation into giant clouds with sizes on the order of its thickness. The gas disk fragmentation in irregular galaxies, where the spirals that synchronize star formation are absent, occurs randomly, thus justifying their name. OB associations and star clusters (closely bound star systems) are arranged hierarchically: associations incorporate clusters. Therefore, their evolution is a single process, which we will proceed to examine. Let us consider a simple criterion for the gravitational instability of a Keplerian gas disk. For instability to occur, it is necessary that the gas density in the disk exceed the disk's tidal density ( $m_g/R^3$ ), or  $H/R < m_g/M$ . Here,  $H$  is the thickness,  $R$  is the radius, and  $m_g$  is the gas disk's mass;  $M$  is the central object's mass (Toomre, 1964) [23].

The process of the gas disk compression toward the Galaxy plane (and an increase in the gas density) is facilitated by gas cooling and the  $Z$ -component of the Galactic gravitational field. Protoclusters with masses of  $(10^2-10^4)M_\odot$  and mass spectrum  $dN/dM \sim M^{-2}$  form in the compressing turbulent gas (Tutukov, 2019) [24]. The characteristic mass of open clusters of our

Galaxy is between 300 and 3000  $M_\odot$  (Trujillo-Gomez et al., 2019) [25].

It is important to note that the efficiency of the transformation of gas into stars does not exceed 30% (Lada and Lada, 2003) [26], so the gas loss due to outflow caused by hydrogen ionization leads to the loss of stars and decay of  $\sim 90\%$  of clusters over a period of  $\sim 10^5$  years (Tutukov, 1978 [27]; Lada and Lada, 2003 [26]). Let us find the maximum mass of the cluster that allows it to survive and not decay completely. The characteristic relationship between the cluster radius and its mass was obtained in [24]:

$$M_{cl} = 0.2R^2, \quad (1)$$

where  $M_{cl}$  is the mass (in grams), and  $R$  is the radius of the cluster (in cm).

Using (1), we find that the characteristic velocity of the stars in the forming clusters  $v \approx 3 \times 10^4 (M_{cl}/M_\odot)^{1/4}$  cm/s. This means that clusters with a mass below  $\sim 10^6 M_\odot$  decay after the loss of gas, because the expansion rate of the ionized hydrogen zone is higher than the characteristic velocity of cluster stars. Thus, the sought-for boundary estimate is the mass of  $10^6 M_\odot$ . This value separates clusters as objects with a single burst of star formation from dwarf galaxies and galactic nuclei. The gravitational potential of the latter is sufficient to retain ionized hydrogen, which recombines and participates in the further process of star formation. The observed correlation of brightness with the size of star systems confirms the existence of a mass boundary between clusters (with a single star formation event) and galaxies with continuous star formation (Simon, 2019) [28].

At the front of a spiral wave in spiral galaxies or randomly in irregular galaxies, the gas component is divided into fragments with sizes of several hundred parsecs and a mass of  $\sim (10^5-10^6)M_\odot$ . The process of gas cooling leads to its fragmentation. As a result of sequential fragmentation, protoclusters with characteristic masses of  $\sim 10^3 M_\odot$  occur. The loss of gas by young clusters under the stellar wind from ionized hydrogen zones leads to the decay of  $\sim 90\%$  young clusters (Tutukov, 1978 [27]; Krumholz and McKee, 2020 [29]). As a result, the OB association is filled with young stars. The absence of gravitational bounds of the OB association leads to its scattering along the orbit around the galaxy center. Over time, a strong stellar stream appears, consisting of the association field stars and streams of surviving star clusters. As a result of the evolution over time of  $\sim 10^9$  years, the stream closes in a ring around the galaxy center. Given a velocity dispersion of  $\sim 30$  km/s (Eubanks, 2019 [30]), the length of the stellar stream—the product of the OB association decay—will be  $\sim 60t_6$  pc, where  $t_6$  is the age of the association in million years (Fig. 1).

Figure 1 shows all the evolutionary stages of clusters (left branch) and OB associations (right branch).

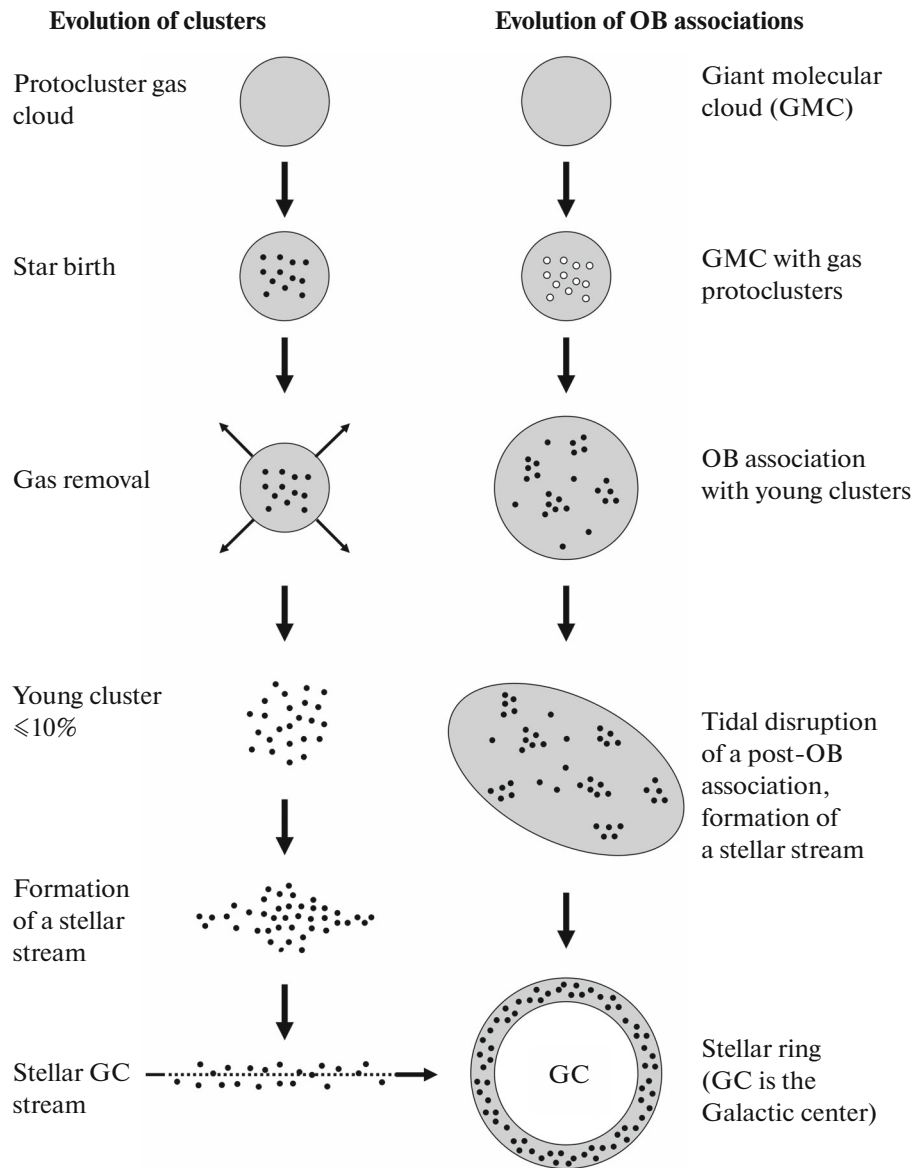


**Fig. 1.** Evolution scenario of star clusters (left branch) and OB associations (right branch). Successive stages of evolution are shown. The dots schematically denote the stellar component, the groups of dots are clusters, and the open circles are protoclusters. The gray color indicates the presence of gas in the system.

Let us turn to the top part of Fig. 1, where the first four steps illustrate the abovementioned processes: the nucleation of two branches of evolution, the beginning of fragmentation at the first stage and further star formation, gas loss, the decay of most clusters, and the origination of stellar streams. As we will see later (Fig. 2), the association gradually extending along the orbit closes in a ring around the galactic center over the Galaxy's lifetime. This time is not sufficient for a cluster, and it reaches only the stage of a stellar stream. Star clusters are the main star formation zones in galaxies, and after gas is removed by ionized hydrogen zones, only a few percent of gravitationally bound

clusters remain (Tutukov, 1978 [27]; Kroupa, 2007 [31]). The decayed clusters fill the volume with stars that inherit the basic parameters of the initial giant molecular clouds. OB associations are not gravitationally bound, so the tidal forces of the Galaxy distort their shape over a period on the order of Keplerian time at the level of the orbit of the association in the Galaxy. We have simulated this process numerically using a simple model (Fig. 2). Thus, tidal forces determine the evolution of the OB association shape, distorting it and eventually turning into a stellar stream that gradually extends to enormous distances ( $\sim 50$  kpc).

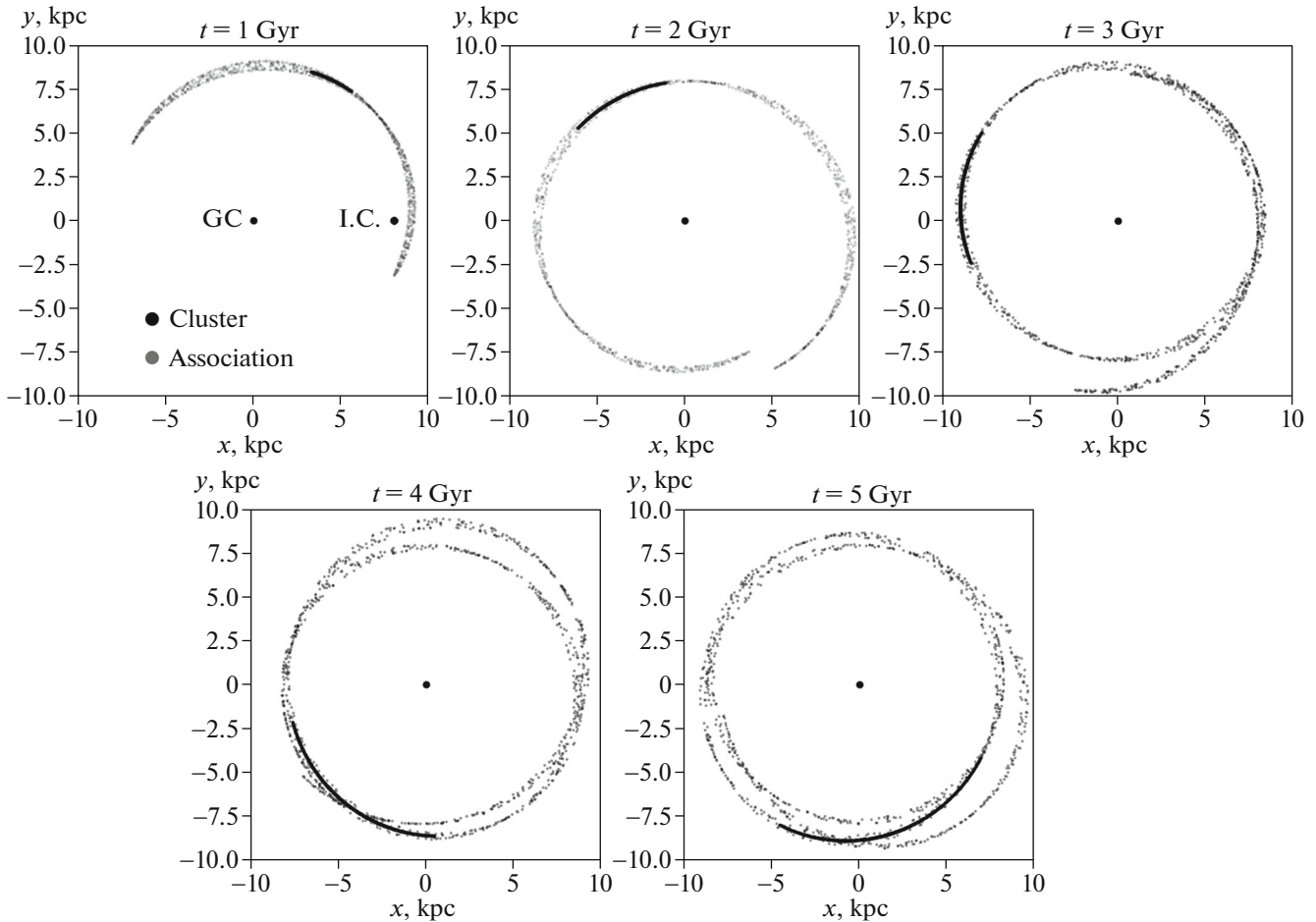


**Fig. 2.** Cloud evolution of 1000 points in projection onto the plane of the galactic disk  $XY$  (a rectangular galactic coordinate system is used). The gray dots in the OB association represent star clusters. The initial position of the cloud is denoted by I.C. (initial conditions). The black dots in the star cluster represent stars. The evolution time is indicated at the top of each panel.

### 3. DECAY OF STAR CLUSTERS

The problem of gradual decay of star clusters as a system of gravitational points with negative total energy was first considered by Eddington [7]. It should be noted that in its full form without significant simplifications, this problem can only be solved numerically, and the solution will depend on a number of not fully defined parameters. The essence of the solution can be understood based on a simple model of a spherical system of  $N$  gravitationally bound points of the same mass  $m$  with a system  $R$  radius. The initial equilibrium of the system allows us to estimate the characteristic velocity of the points  $v = \sqrt{GNm/R}$ ; hereinafter,  $G$  is the gravitational constant. Close passages of the points change their velocity. To change the velocity by an amount on the order of the departure velocity, they have to approach each other at a distance  $r \sim Gm/v^2$ . The characteristic time  $T$  required by the cluster stars for such an encounter is

$$T = T_k N, \quad (2)$$

where  $T_k = R^{3/2}/\sqrt{GNm}$ .

Taking the formula  $R \approx 2(Nm)^{1/2}$  for the cluster radius, as follows from (1) [21], we find that the characteristic time of their evaporation is  $T \approx 3 \times 10^4 N^{5/4}$  years. For clusters, we can take  $N \approx 10^3$ ; the time of their dissipation is then on the order of  $10^8$  years, which is confirmed by the observational estimates made by Gieles and Baumgardt [32].

At the same time, the cause of the stability of massive globular clusters with masses  $(10^5-10^6)M_\odot$  becomes clear. It is known that the lifetime of star clusters grows in proportion to their mass. It follows from (2) that the time of “evaporation” of clusters with masses above  $\sim 3 \times 10^4 M_\odot$  will exceed the Hubble time. Therefore, galactic clusters that survived the initial loss of the gas component remain in the galaxy “forever.” Evaporation of low-mass star clusters leads to the fact that their mass spectrum changes with time due to a decrease in the number of low-mass clusters. The high evaporation rate of clusters due to pairwise

encounters of stars should not be surprising, because the binding energy of clusters is small. A simple estimate shows that at  $R \sim 2M^{1/2}$  (formula (1)), the binding energy of a cluster consisting of  $N$  stars of solar mass is equal to the binding energy of two stars of solar mass in a circular orbit with a semiaxis of  $\sim 10^6 N^{-3/2} R_\odot$  where  $R_\odot$  is the solar radius. It turns out that one contact pair of such stars has an energy equal to that of a cluster with a mass of  $\sim 5 \times 10^3 M_\odot$ . As a result, it is clear that binary stars may actively participate in the evaporation of cluster stars and impart some of the evaporated stars with high spatial velocities reaching hundreds of kilometers per second.

Figure 1 shows this stage at the third step of the evolution of OB associations, in which surviving clusters remain; many of them are observed in the current time period.

## 4. STELLAR STREAMS

### 4.1. Types of Streams

Let us proceed to the lower steps of the evolution scenario in Fig. 1, i.e., to the origination and evolution of stellar streams. Astronomers have paid attention to stellar streams for a long time. Studies in this direction began with Kapteyn's discussion in 1911 of the reality of stellar chains that stand out in the celestial sphere [33]. A few years later, a new model was proposed for their formation as a product of star system decay as a result of pairwise interactions (Jeans, 1916) [34]. Jeans accompanied the description of his simple model with an insightful commentary: "It would be absurd to imagine that the complex phenomena of our Universe could be entirely explained in terms of simple conceptions such as these, but it is perhaps worth investigating whether some of its features may not admit of explanation in this way." Lindblad (1921) [35] supported Jeans' simple model, and Chandrasekhar (1942) [36] explained the dispersion equality of the radial and polar velocities of the stream stars by the symmetry of their initial velocities.

In [37], Ogorodnikov and Latyshev (1968) drew attention to the parameter correlation of a near-solar stellar stream with the positions and parameters of nearby star clusters. Eggen [38] showed that stellar streams contain a significant part of galactic disk stars.

The study of the "evaporation" of star clusters during their quasi-stationary evolution leading to the occurrence of "stellar tails" and the tidal disruption of dwarf galaxies in the gravitational field of massive neighbors has recently gained popularity. Partial or complete destruction of clusters and galaxies leads to the occurrence of stellar streams. These studies are stimulated by the increasing accuracy of the radial velocities of faint stars and the photometric sensitivity of modern galaxy images, which makes it possible to trace stellar streams even far on the periphery of galaxies.

Chumak and Rastorguev (2006, 2008) [39, 40] constructed models for the formation of "stellar tails" of the Pleiades, Hyades, and other clusters due to the evaporation of their stars during the mutual interaction of the stars in these clusters. The analysis of the Palomar 5 stream showed the absence of significant inhomogeneities, which was consistent with the quasi-stationary "evaporation" of stars (Ibata, 2016) [41]. The tidal disruption of globular clusters was studied by Bose (2018) [42], and its dependence on the cluster mass was examined by Balbinot (2018) [43] and Gieles (2018) [44]. Of particular interest was the study of the star cluster  $\omega$  Centauri (NGC 5139), distinguished by a dense and long "stellar tail" (Ibata, 2019) [45]; the chemical composition study of its stars showed that this cluster is a dense nucleus of a dwarf galaxy, absorbed and disrupted by the gravitational field of our Galaxy. Another popular example of a destruction of a Galactic satellite is the stream in Sagittarius: a detailed study of its stars showed that star formation in it ceased several billion years ago (de Boer et al., 2015) [46]. A representative example of the tidal disruption of a low-mass satellite is the galaxy NGC 5387 with a mass of  $\sim 1.1 \times 10^{11} M_\odot$  (Beaton et al., 2014) [47]. The destroyed satellite with a mass  $\sim 4 \times 10^{10} M_\odot$  turned into a bright dense ring around the center of the galaxy NGC 5387.

During the search for the ways of the stellar halo formation of galaxies, Morrison and Olszewski [48] found that stellar streams could take an active part in this process. The tidal disruption of the Galaxy's satellites was taken as the cause of the occurrence of stellar streams in the halo. Later, Yoon et al. [49] showed that stellar streams are non-uniform, which was naturally attributed to the non-uniformity of tidally disrupted galactic satellites. Modeling the destruction of low-mass galaxies in the gravitational field of massive galaxies confirmed these expectations (Naik et al., 2020) [50]. As a result, stellar streams of these two families have become established in astrophysics. Streams in the disk are probable decay products of most star clusters (lower stages of the evolution branch in Fig. 1) and OB associations (right branch in Fig. 1). The second family includes streams in the Galactic halo, which, as we will now see, are the decay products of the Galaxy's satellites. The calculation results illustrating this family are given in Section 5.

### 4.2. Galactic Halo Structure and Streams Generated by Galactic Satellites

Let us consider the modern hypothesis that explains the nature of the galactic halo. The stellar halo of galaxies is a combined product of the early spheroidal stages of their evolution and absorption of nearby smaller satellites (Kruijssen et al., 2020) [51]. The latter process is currently gaining increased attention (Fattahi et al., 2020 [52]; Boltrini et al., 2020

[53]). Recently, a detailed study of structures with low surface brightness located in the vicinity of galaxies has allowed, along with the well-known stellar streams like the Sagittarius Stream (Antoja et al., 2020 [54]; Ibata et al., 2020 [55]), finding similar streams near other nearby galaxies, for example, NGC 5907 (Alabi et al., 2020) [56] and MKn 938 (Afanasyev et al., 2020) [57]. Interestingly, in the stream enveloping NGC 5907, it was possible to identify several globular clusters that belonged to a satellite previously disrupted by tidal forces. The length of this stream is tens of kiloparsecs. As a result of a detailed study of our Galaxy's periphery, Roebler et al. [58] discovered about a hundred satellites in a region with a radius of approximately 100 kpc. Apparently, some of the nearby satellites were previously absorbed by the Milky Way. Recent absorption events are marked by stellar streams; the final result of this process is the stellar halo of the Galaxy, a significant part of the stars which rotate opposite to the Galaxy's rotation (Krugel and Tutukov [59]). Probably, it should be noted that such a mechanism for the formation of the stellar halo of massive galaxies is common.

The decay result of the OB associations in our Galaxy's disk and low-mass satellites in its halo is the occurrence in the Sun's neighborhood of many ellipsoidal stellar structures discovered by Ratzenbock et al. [60] and distinct stellar streams of various length (Riley and Strigari [61], Ibata et al. [62], Arakelyan et al. [63]). Some of these streams demonstrate a distinct structure parametrically bound to known clusters (Eubanks [30]). Ultimately, the observed stellar field of the disk and the halo of our Galaxy and other galaxies is the sum of different-aged stellar streams formed due to the decay of the OB associations and the disruption of nearby galaxy satellites (Duncan, 2020 [64]; Ratcliffe et al., 2020 [65]).

Let us consider the conditions for decay of a satellite galaxy with mass  $m$  and radius  $r$  (recall that  $m = 0.2r^2$  (formula (1)) in the gravitational field of a massive galaxy with a flat rotation curve, mass  $M$ , and radius  $R$ . Let us assume that tidal disruption begins when the satellite is submerged into the galaxy at a distance where its density becomes equal to the average density of the massive galaxy's nucleus. Simple transformations demonstrate that the condition for the beginning of disruption is satisfied when  $M_R/M < (m/M)^{1/4}$ , where  $M_R$  is the nucleus mass of the massive galaxy with an average density equal to the density of the satellite. While relation (1) is maintained, low-mass satellites can penetrate deep into the galactic nucleus region without being disrupted. Obviously, satellites of lower average density (low surface brightness) will be destroyed already at the massive galaxy's periphery. This explains why globular clusters "survive" in the observed stellar streams of our Galaxy and other galaxies (Alabi et al. [56]).

It is important to emphasize that some of the globular clusters that exhibit repeated star formation (Salari et al. [66]) are actually dense nuclei of dwarf galaxies disrupted during mergers with our Galaxy. For example,  $\omega$  Cen is not a globular cluster, but is the nucleus of a dwarf galaxy, as shown by Ibata et al., 2018 [64]. Note that repeated bursts of star formation in the dense nuclei of galaxies are probably common phenomena (Krugel and Tutukov [59]). They differ from globular clusters with a single burst of star formation during the collapse of the initial molecular cloud in that the second burst clears the cluster of the initial gas. Some of the globular clusters of our Galaxy originated in its satellites and, having survived the disruption of the parent galaxies, became members of the galactic halo.

Let us consider the effect of a "reverse" spatial rotation of the stellar population in the halo. The absorption result of nearby low-mass satellites by massive galaxies is the observed retrograde rotation of a noticeable star fraction in the halo of our Galaxy (Koppelman et al., 2019) [68] and probably other galaxies. Using a simple model, we estimate the deceleration time of a point-like object with mass  $m$  in the gravitational field of a massive galaxy with mass  $M$  and a flat rotation curve. The rotation curve defines the distribution of the gravitating matter in the galaxy:

$M_R = v^2 R/G$ , where  $M_R$  is the mass of the galaxy within the radius  $R$ , and  $v$  is the rotation velocity. The tidal deceleration time of an object with mass  $m$  is  $\tau_{fr} = v^3/(G^2\rho m)$ , where  $\rho = M_R/R^3$  is the local average density of the galaxy. The velocity is then  $v = \sqrt{GM_0/R_0}$ , where  $M_0$  and  $R_0$  are the total mass and radius of the galaxy. As a result, the expression  $\tau_{fr} = \tau_k(M_R/M_0)^2 M_0/m$ ,  $\tau_k = 10^8(M/10^{11}M_\odot)$  years, is true for the deceleration time. The last expression clarifies the role of various factors in the satellite deceleration: deceleration intensifies with the immersion of the satellite into the interior and with an increase in the mass of the satellite. It is clear that globular clusters with mass of  $(10^5 - 10^6)M_\odot$  remain in the bulges of their galaxies for the Hubble time.

#### 4.3. Unusual Streams and the Mutual Influence of Galaxies

Among the possible reasons for the appearance of stellar streams in galaxy clusters, it is necessary to mention galaxy collisions in the dense nuclei of clusters. This refers to collisions of gas-rich galaxies with spatial velocities at their edge above parabolic  $(\sim 300(M/10^{11}M_\odot)^{1/4} \text{ km/s})$  [24]. Collisions lead to the loss of the gas component in such galaxies with possible star formation during their merger (Tutukov et al., 2011) [69]. If the mass of the gas component in the galaxy exceeded half the total mass, the disruption of its stellar component leads to the occurrence of a giant

stellar stream in the direction along the galaxy's orbit. In addition, if the star formation conditions in the gas in the merger region are satisfied, a newly formed galaxy may turn out to be unstable and eventually form its own stellar stream. Reliable identification of such streams is not yet possible due to their obviously low spatial density. At the early stages of stellar disk expansion, they can manifest themselves as galaxies of low surface brightness (Kavirai, 2020) [70]. The search for giant stellar streams in galaxy clusters that are not associated with specific galaxies should be given special attention based on the remaining globular star clusters. These streams feed the stellar component of the cluster, which uniformly occupies its volume.

## 5. SIMPLE EVOLUTION MODEL OF ASSOCIATIONS AND STAR CLUSTERS

To visualize the evolution of star clusters and OB associations, we used a simple model of a cloud of  $N = 1000$  point-like stars (clusters). The initial position of the cloud is also set at the point (we assume that the stars do not interact gravitationally with each other). The cloud orbits around the Galactic center (GC), while the constituent point-like objects move at different velocities. In the initial data, the directions of the spatial velocity vectors of the points making up the cloud are evenly distributed over the angles, completely covering the celestial sphere. The cloud can play the role of a star cluster or association depending on the choice of the initial spatial velocities of the points. In other words, the absolute value of the spatial velocity determines the type of the system. In the case of a star cluster, these are stars whose spatial velocities are taken equal to 1 km/s. In the case of an OB association that consists of 1000 clusters, spatial velocities are taken as 10 km/s for each cluster. Thus, by setting the initial coordinates and spatial velocity components of each point, we examine the evolution of a cloud moving in a galactic disk around the GC. The results are presented in Fig. 2. To calculate the orbital parameters and integrate the spatial motion, we used the galpy package [71] written in the Python programming language.

We used the realistic classical Milky Way potential (MWPotential2014 [71]) that best reproduces the observed rotation curve of the Galaxy. It is an axisymmetric potential, in which the Galaxy is represented by a three-component model that includes a halo with a radius of 16 kpc, a disk, and a bulge. The density of matter in the Sun's neighborhood is taken as  $0.10 \pm 0.01 M_{\odot} \text{ pc}^{-3}$ . The total potential includes the disk's potential and spherical (halo) component of the Galaxy: the bulge and the disk are described by the Miyamoto–Nagai expressions [72], and the spherically symmetric spatial distribution of the dark matter density in the halo is described by Navarro–Frenk–White [73].

We used the standard model, in which the Sun is assumed to be at a distance  $R_0 = 8$  kpc from the GC; the disk rotation velocity here is  $V_0 = 220$  km/s. It should be noted that the  $R_0$  value was determined in dozens of publications, the authors of which found justified values in the range of 7.4–8.7 kpc. Malkin [74] investigated the “bandwagon effect,” which leads to selection bias in the data that tend to be close to previously published and expected results. No significant trends were revealed. It turned out to be almost impossible to choose the most significant value of  $R_0$  that would differ from the one that we used in the indicated interval. It should be noted that the most recent studies give values  $V_0 = 232.8 \pm 3$  km/s [75] and  $R_0 = 8.178 \pm 0.013$  kpc [76]. In our calculations, we used the above standard values of these parameters given in [71]. The latter differ slightly from the values recommended as of today, but, as verification has shown, the difference in the above values of  $R_0$  and  $V_0$  has a negligible effect on our results.

The calculation results for a star cluster and OB association presented in Fig. 2 were performed in the interval from 0 to 5 Gyr. As seen in Fig. 2, the clouds gradually stretch in the process of motion, extending slightly and turning into streams. The process occurs due to the adopted initial uniform dispersion of velocity directions. Naturally, the stretching effect is more significant where the velocity is higher, i.e., for OB associations. Since associations, initially consisting of clusters, rapidly evolve and decay. In Fig. 2, they already consist almost entirely of stars. Single surviving clusters may remain in the association. Recall that the general course (scenario) of evolution is schematically shown in Fig. 1. The system as a whole moves around the GC at a speed of 220 km/s. The period of revolution of the Sun (Solar System) about the GC (galactic year) is approximately 250 Myr. The integration period of 5 Gyr comprised approximately 20 revolutions about the GC, both for clusters and associations. This cannot be said about the extension magnitude of these systems along the orbit. As stated at the beginning of this section, we base our considerations on the speed of approximately 1 pc/Myr for clusters and 10 pc/Myr for OB associations (which is easy to show by substituting the appropriate units of measurement). As we see in Fig. 2, the association will stretch for 20 kpc over approximately 1 Gyr. Over approximately 2–2.5 Gyr, the association closes in a ring (Fig. 2). Examples of the observed greatly-extended spatial form of open star clusters can be found in [77]. As shown in our research in Fig. 3, the relatively young cluster IC 2391 undergoes a decay stage. In Fig. 3, the cluster size is noticeably increased along the motion around the GC. Figure 3 is plotted according to the catalog of Postnikova et al. (2019) [77]. The open star cluster IC 2391 (MWSC 1529, omi Vel Cluster) is close ( $\sim 145$  pc [78, 79]) and young (its age is  $(4-5) \times 10^7$  years [80, 81]). Considering stars in a wide range of

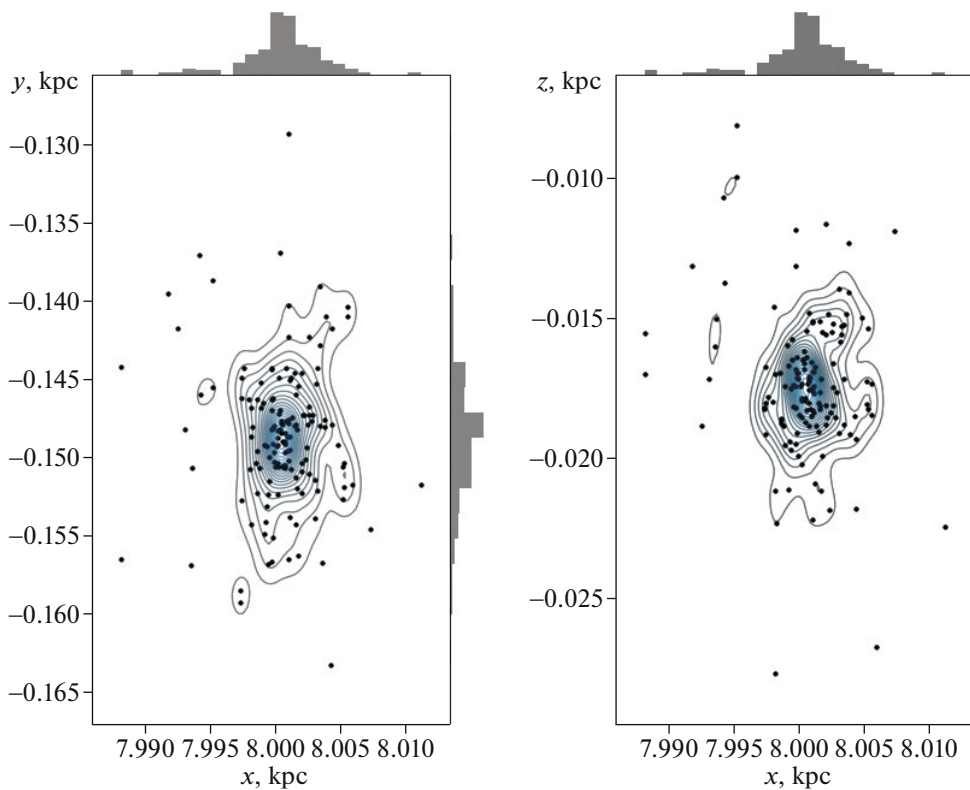


**Fig. 3.** Decay of the cluster IC 2391. The distribution of stars in the galactic plane  $XY$  (left panel) and  $XZ$  (right panel). The equal density levels of stars are shown. The distribution histograms of the number of stars along the corresponding axis are shown above and to the right.

membership probabilities (considering, among others, weakly bound stars or not completely gravitationally related to the cluster) lead to the fact that the cluster begins to stretch along the ordinate axis. In other words, the stars lost by the cluster are spatially stretched along the direction of disk rotation. Possibly, these stars are located in “stellar tails,” as shown in Fig. 2 (in calculations for the cluster). This is evidence of the cluster decay, since the stars of our cloud escape from the clusters uniformly throughout the sphere, and not through the Lagrange points.

As noted by Lodieu et al. (2019) [82], the cluster tails may have an “odd” orientation, not being directed along the spatial orbit. This is possibly not only due to the orbits of the clusters around the GC being noncircular, but also due to significant  $Z$ -amplitudes of orbital oscillations. The IC 2391 cluster with calculations of the orbits was considered in more detail by Postnikova et al. (2020) [83].

Detailed calculations of another model are presented by Chumak and Rastorguev (2006) [84]. They use the assumption that stars gradually leaving the cluster completely lose their gravitational connection with it. Remaining in orbit, they form two plumes: behind and in front of the cluster. For calculations, the authors of [84] used a modification of the NBODY6

software (Aarseth, 2003) [85]. The specific feature of the modification is that the calculations continued even after the star left the cluster (where the forces from the side of the cluster stars were considered negligible and only the forces of the Galaxy’s regular gravitational field were considered). The initial mass of the cluster and the virial radius varied. The processes of stellar evolution and the dynamics of binary and multiple systems were taken into account separately. The external gravitational field of the Galaxy was taken from Miyamoto and Nagai (1975) [72]. It turned out that over 1.5 Gyr, almost all stars in the cluster escape into plumes. The time of decay of the plume under the action of molecular clouds is approximately 1 Gyr. The stars of the plume can be considered as a moving cluster.

Another model is presented by Kharchenko et al. (2009) [86]. Their study showed that under the influence of the tidal forces of the Galaxy, the open star cluster assumes the shape of an ellipsoid with the major axis oriented approximately toward the GC. This happens in the classic way: the existing force field gradient leads to a difference in the forces of attraction (the diametrically opposite force vectors with respect to the cluster’s center pull the nearest part of the cluster toward the GC and push the far part away).



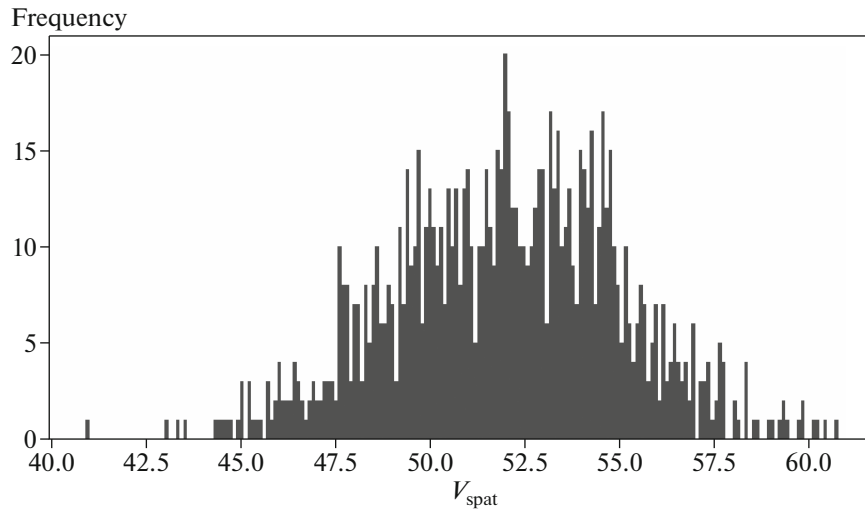


**Fig. 4.** Spatial velocity distribution in the cloud of OB associations of the satellite.

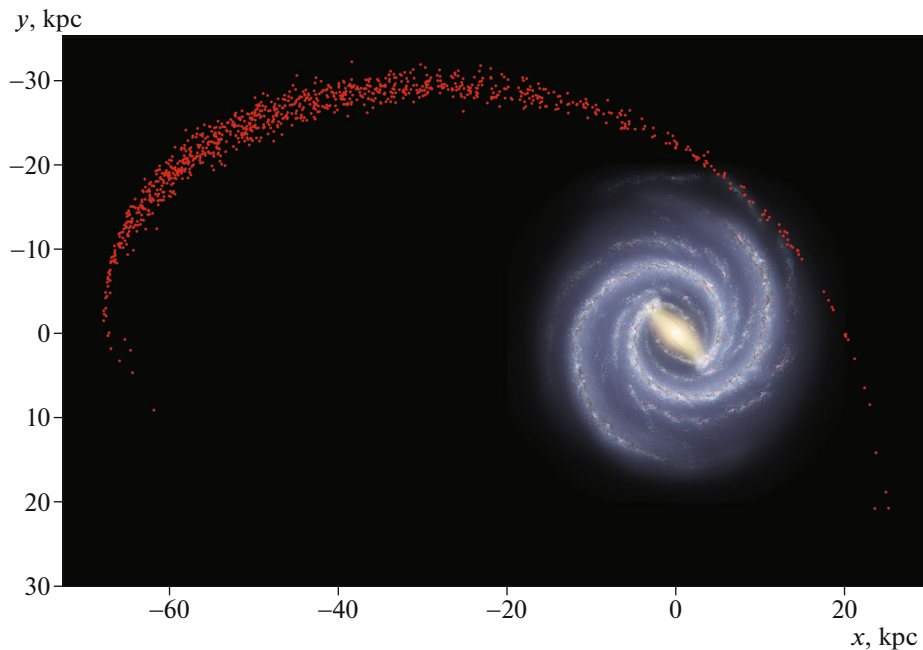


**Fig. 5.** The satellite of the galaxy turns into a stream. The picture corresponds to the time of evolution  $t = 5$  Gyr. The calculations were performed by us (the red dots are decaying star associations ( $N = 1000$ )); the galaxy image is provided by the library for Python and galpy (URL [https://github.com/henrysky/milkyway\\_plot](https://github.com/henrysky/milkyway_plot)).

According to Kepler’s third law, the system most likely slightly rotates about its axis—the far parts of the cluster are forced to move faster in orbit in order to balance the centrifugal force—the cluster does not break apart. Stars that leave clusters form “tails” along the orbit. The calculations in [86] were performed using the  $N$ -body program (fiGRAPE) and the galactic potential from Miyamoto and Nagai (1975) [69]; the star lifetimes and mass loss by stars were considered. The cluster transforms into an ellipsoid, the major axis of

which is oriented at an angle of  $30^\circ$ – $40^\circ$  to the radius vector toward the GC. The observed parameters for 650 clusters were studied. 3D distributions were built only for two clusters (Ursa Major and Hyades); others were considered as projections on the celestial sphere. Note that the ellipsoidal spatial shape of the clusters is very likely determined by the spherical symmetry absence of the initial gas cloud.

It is of interest to apply our simple evolutionary model to a galaxy satellite as well. Within our model,

the satellite of the Galaxy consisting of 1000 OB associations moves in its neighborhood, touching the outer halo or even penetrating deeper at a velocity of  $\sim 250$  km/s. The velocity components are distributed according to a law close to normal, with a peak at 51.5 km/s and a spread of  $3\sigma$ . Thus, the spatial velocity of the components in the satellite takes the values shown in Fig. 4. The results of the calculations of the satellite motion are illustrated in Fig. 5. The classical potential of the Milky Way is used [71]. We can see the motion in a most likely very elongated orbit around the galaxy. The moment of penetration into the outer part of the halo, where the satellite can be observed as a stellar stream in the halo, is clearly visible. It can have a retrograde velocity direction with respect to the rotation of the halo, as discussed in Section 4. The distance of the cloud's orbit from the GC at perihelion is 21 kpc. The calculations are performed in the interval up to 5 Gyr. We see that the satellite, upon leaving the galaxy, gradually turns from an ellipsoidal system into a stream of approximately 30 kpc long. Thus, the results of integrating a simple model presented in Fig. 5—a satellite consisting of 1000 clusters and associations—can be used to interpret observational data.

Dokkum et al. [87] show an observable stream produced by a satellite of the galaxy NGC 5907; the stream is similar to the one obtained in Fig. 5. The resulting shape of the stream is comparable to the stellar stream in the colliding galaxies in the figure shown in [87] (in the center is the spiral galaxy NGC 5907). It should be noted that the study by Shipp et al. [88], which is dedicated to stellar streams discovered with highly sensitive detectors, lists new faint stellar streams at distances up to 50 kpc from the Sun.

## 6. CONCLUSIONS

The presented scenario of the evolution of star clusters and OB associations is a synthesis of modern results of various authors; it provides an understanding of one of the fundamental processes in nature. Figure 1 shows a general scenario for the evolution of star clusters and OB associations up to the Hubble time. Similar processes are observed not only for star clusters, but also for colliding galaxies in the galaxy clusters (Tutukov et al., 2011) [69]. In the nuclei of galaxy clusters, galaxies can lose gas and stars in collisions. A stellar tail with a length of 50 kpc was discovered near the galaxy DDO 44, the satellite of NGC 2019 (Carlin et al., 2019) [89]. The satellite left without gas decays following the same pattern: the action of tidal forces, gradual elongation of stellar streams along the orbits around the center of the galaxy cluster, and a subsequent closure in a ring.

We also add that, judging by the Gaia project results, the time is not far off when each star will receive a “genetic map”, which will reflect its parameters in such detail that it will be possible to establish its “relatives” (“siblings” and “nieces”) from decayed

clusters that initially comprised the same OB association. So far, however, we have to identify streams and ring structures only relying on the observable regions with increased stellar density.

## ACKNOWLEDGMENTS

The study used the software for orbit calculations in the Galaxy created years ago by Bovy [68]. We would like to thank J. Bovy from the Department of Astronomy and Astrophysics at the University of Toronto for his helpful advice, in particular, regarding the use of the galpy package. The authors also thank G.N. Dremova and D.Z. Wiebe for valuable comments and additions. The authors would like to thank the reviewer for helpful comments.

## FUNDING

The study was funded by the Russian Foundation for Basic Research as part of the scientific project no. 20-52-12009. S.V. Vereshchagin and M.D. Sizova are grateful to the Russian Foundation for Basic Research and the German Research Foundation (DFG) for their support.

## REFERENCES

1. Ch. Messier, *Connaissance des Temps ou des Mouvements Célestes* (1781), p. 227.
2. W. Herschel, *Philos. Trans. R. Soc. London* **76**, 457 (1786).
3. J. F. W. Herschel, *Philos. Trans. R. Soc. London* **2**, 274 (1815).
4. J. Dreyer, *Mem. R. Astron. Soc.* **49**, 1 (1888).
5. R. Proctor, *Proc. R. Soc. London* **18**, 169 (1869).
6. W. P. Fleming, *Clusters and Faint Stars*, Vol. 23 of *Harvard College Observatory Observations, Logs, Instrument Readings, and Calculations* (1904–1911).
7. A. S. Eddington, *Mon. Not. R. Astron. Soc.* **71**, 43 (1910).
8. J. Jeans, *Mon. Not. R. Astron. Soc.* **74**, 109 (1913).
9. H. Shapley, *Harvard College Observ. Bull.* **874**, 4 (1930).
10. S. Chandrasekhar, *Astrophys. J.* **97**, 255 (1943).
11. A. S. Eddington, *Nature (London, U.K.)* **106** (2653), 14 (1920).
12. G. Gamow, *Astrophys. J.* **87**, 206 (1938).
13. M. Schwarzschild, *Leaflets Astron. Soc. Pacif.* **5**, 400 (1949).
14. C. M. Bondi and H. Bondi, *Mon. Not. R. Astron. Soc.* **111**, 397 (1951).
15. F. Zwicky, *Publ. Astron. Soc. Pacif.* **72**, 365 (1960).
16. W. Herschel, *Phil. Trans. R. Soc. London* **81**, 71 (1791).
17. J. H. Jeans, *Phil. Trans. R. Soc. London, Ser. A* **199**, 1 (1902).
18. F. Hoyle, *Astrophys. J.* **118**, 513 (1953).

19. A. Blaauw, *Publ. Kapteyn Astron. Lab.* **51**, 1 (1946).
20. W. A. Ambarzumjan, in *Stern-Assoziationen Abhandlungen aus der Sowjetischen Astronomie, Folge 1* (Otto Singer, 1951), p. 33.
21. F. Zwicky, *Phys. Today* **6**, 7 (1953).
22. S. Perlmutter, M. Turner, and M. White, *Phys. Rev. Lett.* **83**, 670 (1999).
23. A. Toomre, *Astrophys. J.* **139**, 1217 (1964).
24. A. V. Tutukov, *Astron. Rep.* **63**, 79 (2019).
25. S. Trujillo-Gomez, M. Reina-Campes, and J. Kruijssen, *Mon. Not. R. Astron. Soc.* **488**, 3972 (2019).
26. C. Lada and E. Lada, *Ann. Rev. Astron. Astrophys.* **41**, 57 (2003).
27. A. V. Tutukov, *Astron. Astrophys.* **70**, 57 (1978).
28. J. Simon, *Ann. Rev. Astron. Astrophys.* **57**, 375 (2019).
29. M. Krumholz and C. McKee, *Mon. Not. R. Astron. Soc.* **494**, 624 (2020).
30. T. Eubanks, arXiv: 1912.12730 (2019).
31. P. Kroupa, in *Proceedings of IAU Symposium 241*, Ed. by A. Vazdekis and R. F. Peletier (Cambridge Univ. Press, Cambridge, 2007), p. 109.
32. M. Gieles and H. Baumgardt, *Mon. Not. R. Astron. Soc.* **389**, L1 (2008).
33. J. Kapteyn, *Kon. Nederl. Akad. Wetensch. Proc.* **14**, 524 (1911).
34. J. Jeans, *Mon. Not. R. Astron. Soc.* **76**, 552 (1916).
35. B. Lindblad, *Astrophys. J.* **62**, 191 (1925).
36. S. Chandrasekhar, *Principles of Stellar Dynamics* (Univ. Chicago Press, Chicago, 1942).
37. K. F. Ogorodnikov and I. N. Latyshev, *Sov. Astron.* **12**, 279 (1968).
38. O. Eggen, *Astron. J.* **112**, 1595 (1996).
39. Y. Chumak and A. Rastorguev, *Astron. Lett.* **32**, 446 (2006).
40. Y. Chumak and A. Rastorguev, *IAU Symp.* **246**, 107 (2008).
41. R. Ibata, G. Lewis, and N. Martin, *Astrophys. J.* **819**, 11 (2016).
42. S. Bose, I. Ginsburg, and A. Loeb, *Astrophys. J.* **859**, 13 (2018).
43. E. Balbinot, M. Gieles, *Mon. Not. R. Astron. Soc.* **474**, 2479 (2018).
44. M. Gieles, C. Charbonnel, M. G. H. Krause, et al., *Mon. Not. R. Astron. Soc.* **478**, 2 (2018).
45. R. Ibata, M. Bellazzini, and K. Melhan, *Nat. Astron.* **3**, 667 (2019).
46. T. de Boer, V. Belokurov, and S. Koposov, *Mon. Not. R. Astron. Soc.* **451**, 3489 (2015).
47. R. Beaton, D. Martinez-Delgado, S. Majewski, et al., *Astrophys. J.* **790**, 117 (2014).
48. H. Morrison, M. Mario, and E. Olszewski, *ASP Conf. Proc.* **273**, 123 (2002).
49. J. Yoon, K. Johnston, and D. Hogg, *Astrophys. J.* **731**, 15 (2011).
50. A. P. Naik, N. W. Evans, E. Puchwein, H. Zhao, and A. C. Davis, arXiv: 2002.05738 (2020).
51. J. M. Diederik Kruijssen, J. L. Pfeffer, M. Chevance, A. Bonaca, et al., arXiv: 2003.01119 (2020).
52. A. Fattahi, A. Deason, and C. Frenc, arXiv: 2002.12043 (2020).
53. P. Boltrini, R. Mohayaee, and J. Silk, arXiv: 2002.12192 (2020).
54. T. Antoja, P. Rames, C. Mateo, et al., arXiv: 2002.10012 (2020).
55. R. Ibata, M. Bellazzini, G. Thomas, K. Malhan, N. Martin, B. Famaey, and A. Siebert, *Astrophys. J. Lett.* **891**, 1 (2020).
56. A. Alabi, D. A. Forbes, A. J. Romanowsky, and J. P. Brodie, *Mon. Not. R. Astron. Soc.* **491**, 5693 (2020).
57. V. Afanasiev, A. Moiseev, and A. Smirnova, *Astrophys. Bull.* **75**, 12 (2020).
58. E. Roebler, R. Buscicchio, and A. Vecchio, arXiv: 2002.10465 (2020).
59. E. Krugel and A. V. Tutukov, *Astron. Astrophys.* **275**, 416 (1993).
60. S. Ratzenbock, S. Meingast, J. Alves, T. Möller, and I. Bomze, arXiv: 2002.05728 (2020).
61. A. Riley and L. Strigari, *Mon. Not. R. Astron. Soc.* **494**, 983 (2020).
62. R. Ibata, K. Malhan, N. Martin, and E. Starckenburg, *Astrophys. J.* **865**, 85 (2018).
63. N. Arakelyan, S. Pilipenko, and N. Libeskind, *Mon. Not. R. Astron. Soc.* **481**, 918 (2018).
64. A. Duncan, *Mon. Not. R. Astron. Soc.* **493**, 847 (2020).
65. B. Ratcliffe, M. Neiss, K. Johnston, and B. Sen, arXiv: 2002.07183 (2020).
66. M. Salaris, S. Cassisi, A. Mucciarelli, and D. Nardiello, *Astron. Astrophys.* **629**, 6 (2019).
67. R. Ibata, K. Malhan, and N. Martin, *Astrophys. J.* **872**, 23 (2019).
68. H. Koppelman, A. Helmi, D. Massari, A. M. Price-Whelan, and T. K. Starckenburg, *Astron. Astrophys.* **631**, L9 (2019).
69. A. V. Tutukov, G. Lazareva, and I. Kulikov, *Astron. Rep.* **55**, 770 (2011).
70. S. Kavirai, arXiv: 2001.01728 (2020).
71. J. Bovy, *Astrophys. J. Suppl. Ser.* **216**, 2 (2015).
72. M. Miyamoto and R. Nagai, *Publ. Astron. Soc. Jpn.* **27**, 533 (1975).
73. J. Navarro, C. Frenk, and S. White, *Astrophys. J.* **462**, 563 (1996).
74. Z. M. Malkin, *Astron. Rep.* **57**, 128 (2013).
75. P. J. McMillan, *Mon. Not. R. Astron. Soc.* **465**, 1 (2017).
76. R. Abuter, A. Amorim, M. Bauböck, J. P. Berger, et al. (Gravity Collab.), *Astron. Astrophys.* **625**, L10 (2019).
77. E. S. Postnikova, N. V. Chupina, and S. V. Vereshchagin, *INASAN Sci. Rep.* **3**, 336 (2019).
78. N. Robichon, Y. Lebreton, and F. Arenou, *Astrophys. Space Sci.* **265**, 279 (1999).

79. R. J. Dodd, *Mon. Not. R. Astron. Soc.* **355**, 959 (2004).
80. D. Barrado y Navascués, J. R. Stauffer, and R. Jayawardhana, *Astrophys. J.* **614**, 386 (2004).
81. I. Platais, C. Melo, J.-C. Mermilliod, V. Kozhurina-Platais, J. P. Fulbright, R. A. Méndez, M. Altmann, and J. Sperauskas, *Astron. Astrophys.* **461**, 509 (2007).
82. N. Lodieu, A. Pérez-Garrido, R. L. Smart, and R. Silvotti, *Astron. Astrophys.* **628**, A66 (2019).
83. E. S. Postnikova, W. H. Elsahoury, D. P. Sariya, N. V. Chupina, S. V. Vereshchagin, and I.-G. Jiang, *Res. Astron. Astrophys.* **20**, 2 (2020).
84. Ya. O. Chumak and A. S. Rastorguev, *Astron. Lett.* **32**, 3 (2006).
85. S. J. Aarseth and J. Sverre, *Gravitational N-Body Simulations* (Cambridge Univ. Press, Cambridge, 2003).
86. N. V. Kharchenko, P. Berczik, M. I. Petrov, A. E. Piskunov, S. Röser, E. Schilbach, and R.-D. Scholz, *Astron. Astrophys.* **495**, 3 (2009).
87. P. van Dokkum, C. Gilhuly, A. Bonaca, A. Merritt, et al., *Astrophys. J. Lett.* **883**, 2 (2019).
88. N. Shipp, A. Drlica-Wagner, E. Balbinot, P. Ferguson, et al., *Astrophys. J.* **862**, 114 (2018).
89. J. L. Carlin, C. T. Garling, A. H. G. Peter, D. Crnojević, et al., *Astrophys. J.* **886**, 11 (2019).

*Translated by M. Chubarova*